ORIGINAL PAPER

Synthesis and characterization of 5 V $LiCo_xNi_yMn_{2-x-y}O_4$ ($x = y = 0.25$) cathode materials for use in rechargeable lithium batteries

S. Rajakumar · R. Thirunakaran · A. Sivashanmugam · Jun-ichi Yamaki · S. Gopukumar

Abstract Double doped spinel $LiCo_xNi_yMn_{2-x-y}O_4$ ($x = y = 0.25$) have been synthesised via sol–gel method using different chelating agents viz., acetic acid, maleic acid and oxalic acid to obtain 5 V positive electrode material for use in lithium rechargeable batteries. The sol–gel route endows lower processing temperature, lesser synthesis time, high purity, better homogeneity, good control of particle size and surface morphology. Physical characterizations of the synthesized powder were carried out using thermo-gravimetric and differential thermal analysis (TG/DTA), X-ray diffraction (XRD), scanning electron microscopy (SEM) and Fourier transform infrared spectroscopy (FTIR). The electrochemical behaviour of the calcined samples has been carried out by galvanostatic charge/discharge cycling studies in the voltage range 3–5 V. The XRD patterns reveal crystalline single-phase spinel product. SEM photographs indicate micron sized particles with good agglomeration. The charge–discharge studies show $LiCo_{0.25}Ni_{0.25}Mn_{1.5}O_4$ synthesized using oxalic acid to be as a promising cathode material as compared to other two chelating agents and delivers average discharge capacity of 110 mA h g^{-1} with low capacity fade of 0.2 mA h g^{-1} per cycle over the investigated 15 cycles.

1 Introduction

Miniaturization of electronics and the demand of effective electrochemical power sources necessitate high performing lithium secondary batteries. A major impetus is to find out cheaper cathode materials than $LiCoO_2$ which is used in majority of commercial lithium batteries. Moreover, there is a strong initiative to develop materials of better rate capability and high voltage, than the existing available materials ($LiCoO_2$, $LiNiO_2$ and $LiMn_2O_4$). Towards this goal, recent investigations are focused on the development and characterization of cathode materials capable of working in the 5 V zone [1, 2]. The use of $LiCoO_2$ delivers only 50% of its theoretical capacity (273.8 mA h g^{-1}) corresponding to 0.5 lithium extraction. Further, the toxicity of cobalt and since these cells does not work at high voltages (>4.5 V) thereby posing serious problem [3]. Pure phase $LiNiO_2$ is difficult to synthesize because of its tendency to undergo non-stoichiometric reactions and structural instability leads to poor cycling performance and therefore is not the preferred material for commercialization [4]. $LiMn_2O_4$ is considered as a prospective positive electrode material considering its ease of synthesis, low price, abundance and environmentally benign nature. However, the commercial utilization of $LiMn_2O_4$ is hindered by capacity fade upon prolonged cycling especially at elevated temperatures [4–7]. The mechanism of capacity fade has been attributed to various factors viz., Jahn–Teller distortion [8, 9], lattice instability [10], manganese dissolution [8], lattice site exchange between lithium and manganese ions [11], oxygen rich spinels [12].

S. Rajakumar · R. Thirunakaran · A. Sivashanmugam · S. Gopukumar (✉)
Central Electrochemical Research Institute (CSIR), Karaikudi 630 006, Tamil Nadu, India
e-mail: deepika_41@rediffmail.com

J. Yamaki
Institute for Materials Chemistry and Engineering, Kyushu University, 6-1 Kasuga-koen, Kasuga 816-8580, Japan

The systematic research has been revealed that partial substitution of Mn in $LiMn_2O_4$ with 3d transition elements like Ni, Co, Cr, Cu, Fe, Ti, and Zn makes it as a 5 V cathode material [13, 14]. Several authors investigated single and multi doped manganese based spinels synthesized by using various chelating agents in order to improve the electrochemical performance [15–21]. Sebastien et al. [22] reported that Ni substitution in $LiMn_2O_4$ for Mn was beneficial for improving the charge/discharge cycling performance in the cut-off voltage 3.5–4.9 V. Gao et al. [23] had already reported that lithium extraction from $LiNi_{0.5}Mn_{1.5}O_4$ takes place at 4.7 V where Ni^{2+} is oxidized to Ni^{4+}. The nickel in the $LiNi_{0.5}Mn_{1.5}O_4$ spinel can reversibly transform from Ni^{2+} to Ni^{4+} during cycling thereby making it possible to replace Mn^{3+} with a small quantity of other transitional metals and elevate the operation potential of the material.

$LiMn_{1.5}Ni_{0.5}O_4$ improves the structure stabilization and capacity retention after prolonged cycling [24] rather than $LiMn_2O_4$. The strive for delivering a high voltage cathode material capable of reduced phase transition during charging and discharging so as to prevent cation disordering and better capacity retention entail partial substitution of Co^{2+}/Co^{3+} in $LiMn_{1.5}Ni_{0.5}O_4$ [24–26]. The present work reports the synthesis, physical and electrochemical characterization of $LiCo_{0.25}Ni_{0.25}Mn_{1.5}O_4$ using chelating agents such as acetic acid, maleic acid and oxalic acid.

2 Experimental section

The flow chart shown in Fig. 1 presents the typical procedures followed for the synthesis of spinel $LiCo_{0.25}Ni_{0.25}Mn_{1.5}O_4$ by sol–gel method using acetic acid, maleic acid and oxalic acid as chelating agents. Stoichiometric proportions of high purity acetates of lithium, manganese, nickel, and cobalt were homogeneously stirred, mixed and dissolved in triple distilled water. The solution was stirred continuously with gentle heating and either of 1 M acetic acid or 1 M maleic acid or 1 M oxalic acid as chelating agent is added drop wise to get a homogeneous solution. The pH of the solution was maintained between 5 and 7.5 and the solution was slowly heated until a viscous gel has been obtained. The gel mass was dried overnight in a hot air oven at 110 °C to obtain a dried mass.

2.1 Physical characterization

A portion of the gel precursors were characterized by thermo-gravimetric and differential analysis (TG/DTA) [PL Thermal Sciences Instrument, model STA 1500] to ascertain the thermal behavior. About 50 mg of the samples were taken and heated in a heating ramp at 20 °C min^{-1} in air. The dried mass was ground well and calcined at different temperatures viz., 250, 400, 600 and 850 °C for 6 h in alumina crucibles and subjected to physical and

Fig. 1 Flow chart for the synthesis of spinel $LiCo_{0.25}Ni_{0.25}Mn_{1.5}O_4$ by sol–gel method using acetic acid, maleic acid and oxalic acid as chelating agents
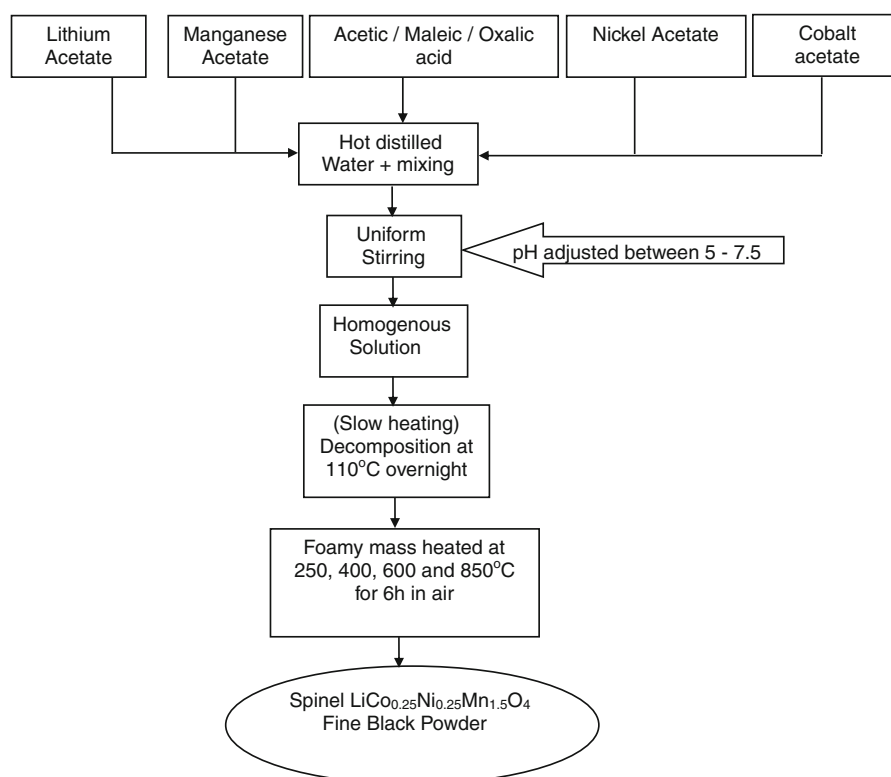
electrochemical studies.The physical characterization of the synthesized samples were carried out by X-ray diffraction (XRD) [JOEL 8030 X-ray diffraction with nickel filtered Cu Kα radiation], Scanning electron microscopy (SEM) [Hitachi S-3000 H], Fourier-transform infrared spectroscopy (FTIR) [Perkin-Elmer, model Paragon-500 spectrophotometer] and finally electrochemical cycling studies.

2.2 Electrochemical cell assembly

The charge/discharge studies were carried out using 2016 coin cell [Hohsen Co., Japan]. Lithium foil has been used as anode, Celgard 2400 as separator and 1 M LiPF$_6$ in 50:50 (v/v) mixture of ethylene carbonate (EC) and diethylene carbonate (DEC) as electrolyte. The cathode has been prepared by a slurry coating procedure. The cathode slurry consisted of 85 wt% of the synthesized material, 10 wt% conducting carbon and 5 wt% polyvinylidienefluride (PVdF) binder dissolved in n-methyl-2-pyrrolidone (NMP). The slurry was coated over aluminium foil and vacuum dried at 110 °C for 2 h. The dried coating was pressed under 10 tonnes load for 2 min, from which electrodes (16 mm diameter) were punched for using as cathode. All cell assembly was done in an argon filled glove box [MBraun, Germany] with <2 ppm oxygen and moisture. The galvanostatic cycling studies were carried out between 3 and 5 V at 0.1 C rate.

3 Results and discussion

3.1 Thermal studies

TG/DTA curves are presented for the synthesis of LiCo$_{0.25}$Ni$_{0.25}$Mn$_{1.5}$O$_4$ using acetic acid, maleic acid and oxalic acid (Fig. 2a–c). The LiCo$_{0.25}$Ni$_{0.25}$Mn$_{1.5}$O$_4$ synthesized via acetic acid as a chelating agent shown in (Fig. 2a) depicts lower weight loss (15%) at the first zone up to 100 °C followed by high weight loss of 30% in the second zone. A broad exothermic peak is observed at 311 °C indicating the formation of the compound. Further, in the case of maleic acid assisted synthesized LiCo$_{0.25}$Ni$_{0.25}$Mn$_{1.5}$O$_4$ (Fig. 2b), two weight loss zones corresponding to 40% up to 200 °C is due to the removal of water molecules and precursors. DTA curve shows a very sharp profile centered at ∼200 °C which is the lowest temperature than in the case of acetic and oxalic acid for the equal stoichiometric dopant ratio of cobalt and nickel. The inactive thermal region is also seen after 200 °C and is the lowest than all the above mentioned TG/DTA curves. It is interesting to observe that in the case of oxalic acid assisted LiCo$_{0.25}$Ni$_{0.25}$Mn$_{1.5}$O$_4$ (Fig. 2c) possesses first
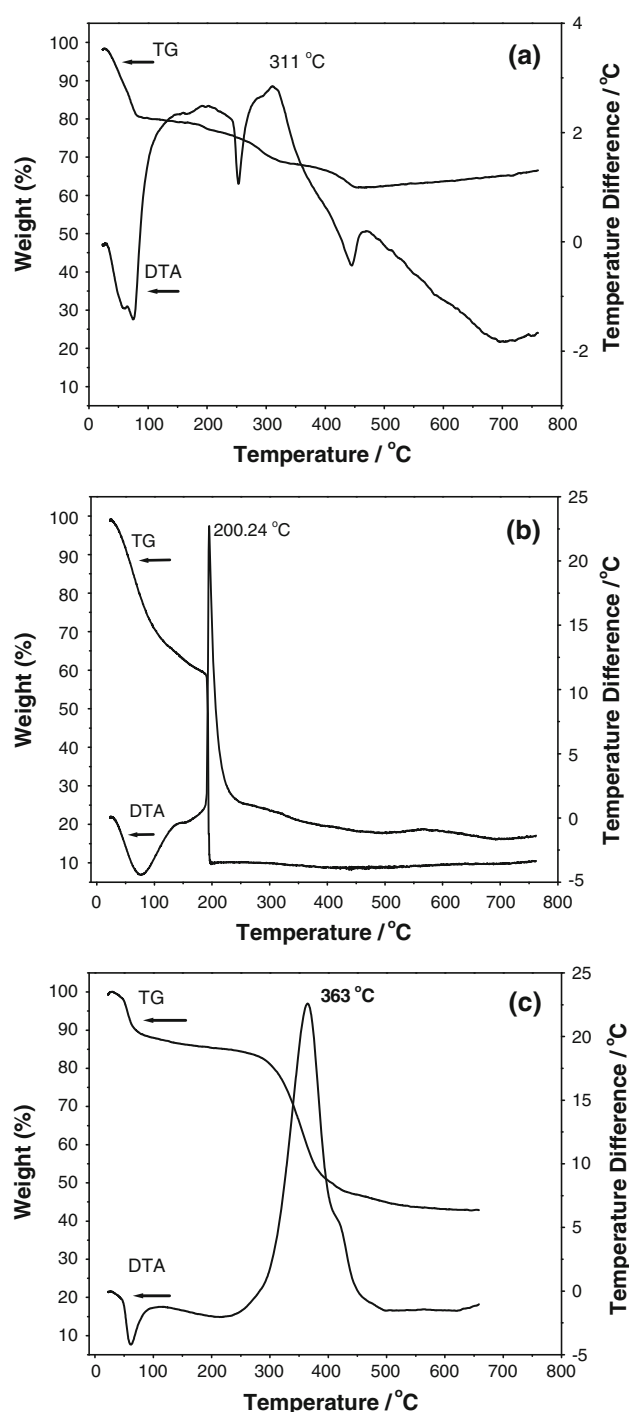
Fig. 2 TG/DTA curves of LiCo$_{0.25}$Ni$_{0.25}$Mn$_{1.5}$O$_4$ using **a** acetic acid, **b** maleic acid and **c** oxalic acid as chelating agents
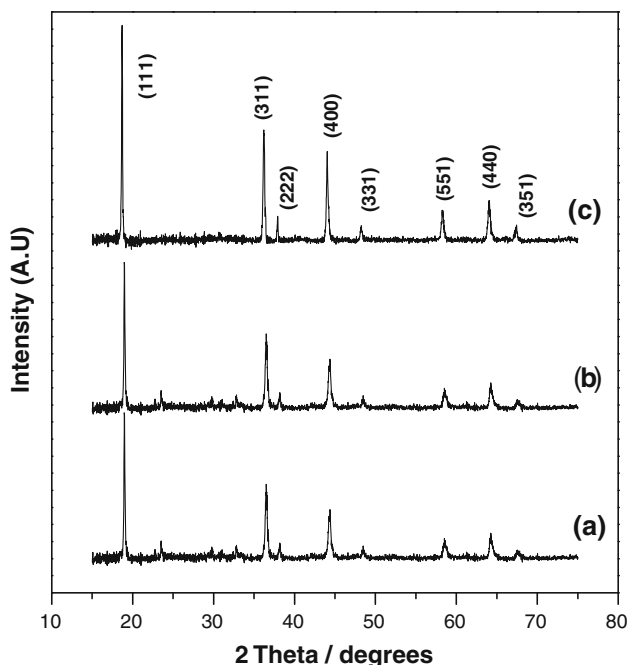
weight loss zone (10%) up to 100 °C and showing a broad exothermic peak at 363 °C for the formation of spinel compound. In this case, further thermal reactions ceases beyond 500 °C which is very high formation temperature compared to all the investigated chelating agents.

3.2 X-ray diffraction

Figure 3a–c shows XRD patterns of the equal stoichiometric composition of cobalt and nickel synthesized using acetic acid (Fig. 3a), maleic acid (Fig. 3b) and oxalic acid (Fig. 3c) assisted $LiCo_xNi_yMn_{2-x-y}O_4$ ($x = y = 0.25$) calcined at 850 °C. It can be seen from these figures that all the signature peaks viz., (111), (311), and (400) are well-defined and are of high intensity suggesting the formation of spinel structure with high degree of crystallinity and phase pure. Furthermore, Fig. 3b and c show similar trend and is in good agreement with previous researchers [27, 28], and JCPDS card No. 35-782. Therefore, as is evident from the above XRD patterns, the pristine spinel has an $Fd3m$ space group wherein lithium occupies the 8a tetrahedral sites while manganese (Mn^{3+} and Mn^{4+}), cobalt (Co^{2+}) and nickel (Ni^{2+}) ions occupies the 16d sites with O^{2-} in the $32e^-$ site [29]. The lattice parameters of $LiCo_{0.25}Ni_{0.25}Mn_{1.5}O_4$ compounds are shown in Table 1.

3.3 FTIR spectroscopy

Figure 4 shows FTIR spectra of the synthesized $LiCo_xNi_yMn_{2-x-y}O_4$ calcined at 850 °C for (a) Co–0.25; Ni–0.25 (acetic acid), (b) Co–0.25; Ni–0.25 (maleic acid) and (c) Co–0.25; Ni–0.25 (oxalic acid). The synthesized samples were ground, mixed with KBr and pressed to pellets of 10 mm diameter. The FTIR spectra reveal stretching and bending vibration of the spinel lithium

Table.1 Lattice parameters of $LiCo_{0.25}Ni_{0.25}Mn_{1.5}O_4$ compounds

| Sample	Chelating agent	a (Å)	V (Å)
$LiCo_{0.25}Ni_{0.25}Mn_{1.5}O_4$	Acetic acid	8.215	554.3
$LiCo_{0.25}Ni_{0.25}Mn_{1.5}O_4$	Maleic acid	8.209	553.1
$LiCo_{0.25}Ni_{0.25}Mn_{1.5}O_4$	Oxalic acid	8.203	552.9
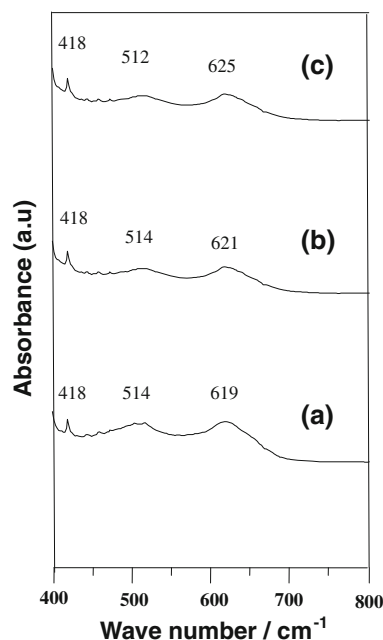
Fig. 4 FTIR spectra of $LiCo_{0.25}Ni_{0.25}Mn_{1.5}O_4$ using (a) acetic acid, (b) maleic acid and (c) oxalic acid as chelating agents

manganese oxide. In the FTIR profile, three peaks are seen at around 418, 510, and 619 cm^{-1} respectively. FTIR studies on cobalt, nickel, multi cations magnesium and nickel doped spinel had been investigated by several authors [30, 31]. The IR spectral band seen at higher wave length between 619 and 625 cm^{-1} which could be attributed both to Co–O and Mn–O stretching vibration [32] and another band at a wave number between 510 and 524 cm^{-1} assigned to Ni–O. These observations are in good accordance with the earlier reports. Further, the FTIR profile seen at lower wave number around 418 cm^{-1} can be assigned to Li–O bending vibration.

3.4 Scanning electron microscopy

Figure 5a–c shows SEM images of the acetic acid, maleic acid and oxalic acid assisted $LiCo_{0.25}Ni_{0.25}Mn_{1.5}O_4$ calcined at 850 °C. The surface morphology of acetic acid assisted $LiCo_{0.25}Ni_{0.25}Mn_{1.5}O_4$ compound (Fig. 5a), small particles are seen with particle size of 1 μm. Further, maleic acid assisted $LiCo_{0.25}Ni_{0.25}Mn_{1.5}O_4$ (Fig. 5b) have ice cube morphology and possesses particle size around

Fig. 3 XRD patterns of $LiCo_{0.25}Ni_{0.25}Mn_{1.5}O_4$ using (a) acetic acid, (b) maleic acid and (c) oxalic acid as chelating agents
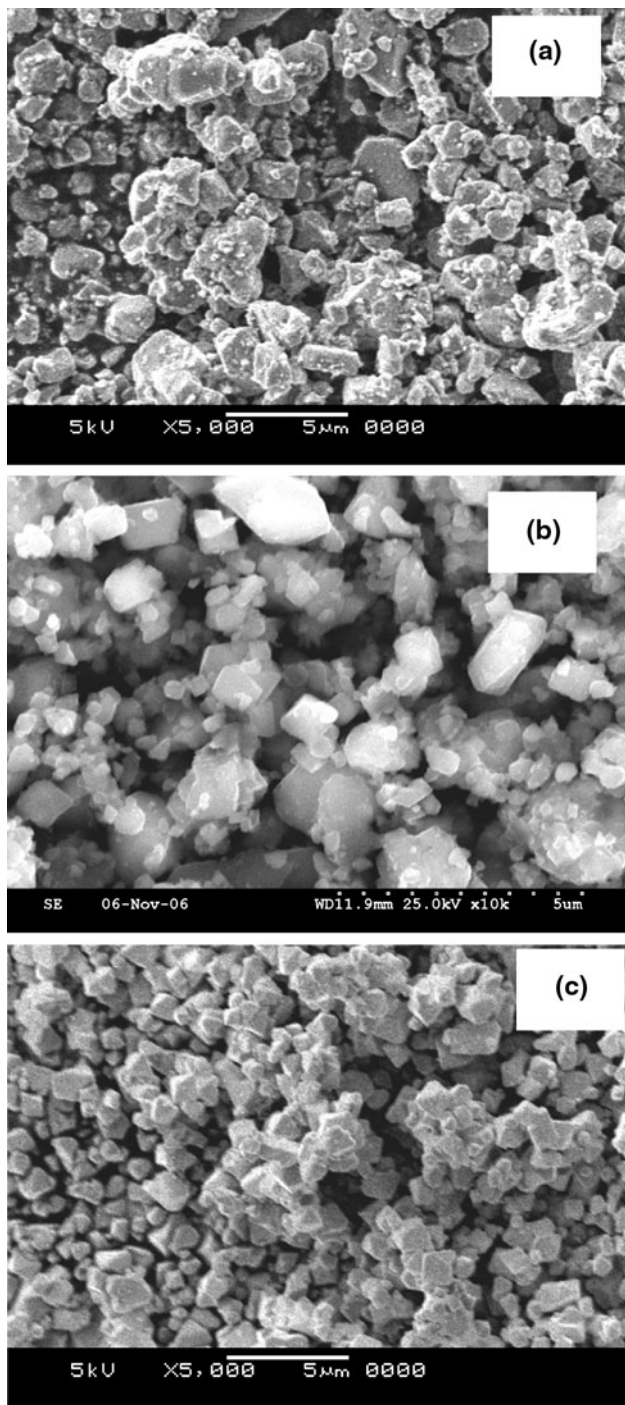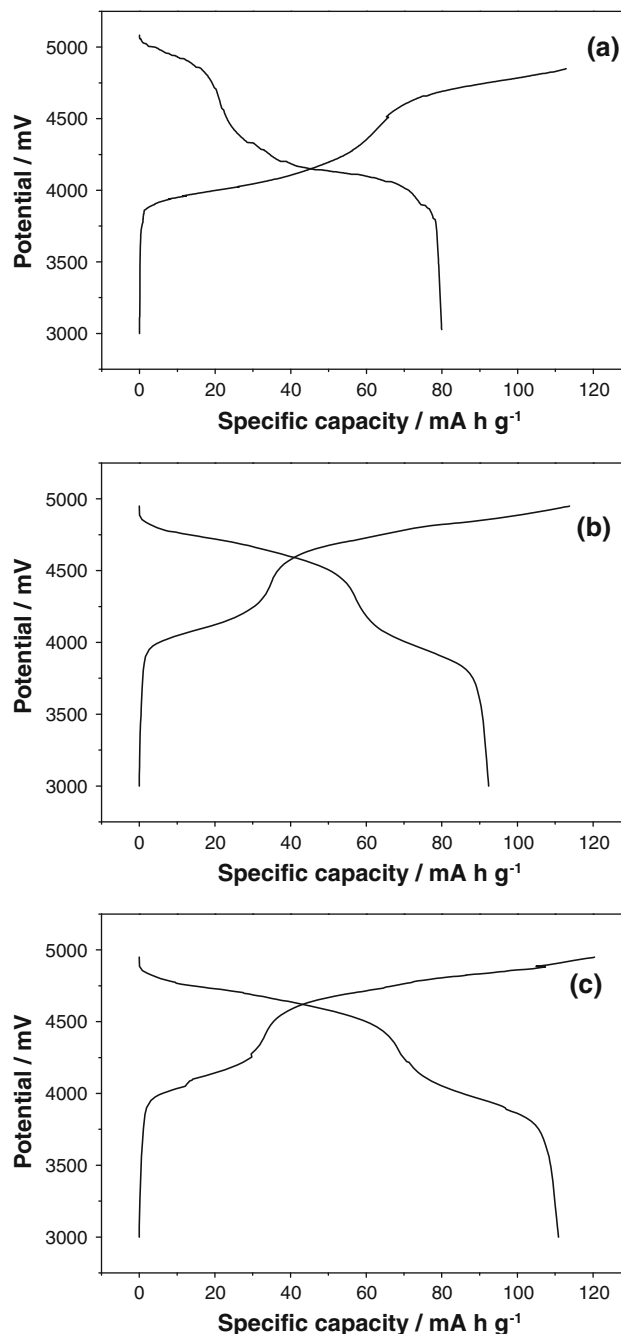
Fig. 5 SEM images of $LiCo_{0.25}Ni_{0.25}Mn_{1.5}O_4$ using **a** acetic acid, **b** maleic acid and **c** oxalic acid as chelating agents

0.8 μm. Lastly, oxalic acid assisted $LiCo_{0.25}Ni_{0.25}Mn_{1.5}O_4$ (Fig. 5c), depicts an average micron sized particles of less than 0.5 μm, which is lower than that of the other two investigated chelating agents assisted particles and also possessing good agglomeration thereby enhancing the inter particle contact for easy lithium ion diffusion.

3.5 Charge–discharge studies

Figure 6a–c shows first cycle charge–discharge curves of sol–gel derived $LiCo_{0.25}Ni_{0.25}Mn_{1.5}O_4$ calcined at 850 °C using all the three chelating agents like acetic acid, maleic acid and oxalic acid. The equal dopant ratio of $LiCo_{0.25}Ni_{0.25}Mn_{1.5}O_4$ using acetic acid, exhibits a maximum discharge capacity of 80 mA h g^{-1} against the charging capacity of 110 mA h g^{-1}. Furthermore, maleic acid and oxalic acid

Fig. 6 First cycle charge–discharge curves of sol–gel derived $LiCo_{0.25}Ni_{0.25}Mn_{1.5}O_4$ using **a** acetic acid, **b** maleic acid and **c** oxalic acid as chelating agents

assisted spinels ($LiCo_{0.25}Ni_{0.25}Mn_{1.5}O_4$), deliver discharge capacities of 92 and 110 mA h g^{-1} respectively. In the sol–gel method, a sol, which is a suspension of small particulates dispersed in a liquid phase, is transformed into a three-dimensional polymeric network viscous gel. In this present work with acetic acid, maleic acid and oxalic acid as chelating agent, the acetic acid is one of the simplest carboxylic acid with one COOH group. The dicarboxylic acids maleic acid and oxalic acid performed better than acetic acid. The maleic acid assisted delivered first discharge capacity of 92 mA h g^{-1} against the charging capacity of 112 mA h g^{-1}. The influence of the acids on the electrochemical characteristics of the final products is compared in terms of the number, n, of –(CH2)– groups between the two carboxylic acid groups in their formulae. Among all the three investigated chelating agents, oxalic acid, the saturated linear aliphatic dicarboxylic acid contains two COOH groups leading to better chelation and active combustion which obviously facilitate high order of grain size and disintegration. These observations are well corroborated by the SEM image (Fig. 5c) and higher formation temperature of the spinel in the TG/DTA curve (Fig. 2c).

Figure 7 presents the cycling behaviour and corresponding columbic efficiencies (CE) of sol–gel derived $LiCo_{0.25}Ni_{0.25}Mn_{1.5}O_4$ calcined at 850 °C synthesized using different chelating agents viz. acetic acid, maleic acid and oxalic acid. Cycling performance of acetic acid assisted $LiCo_{0.25}Ni_{0.25}Mn_{1.5}O_4$ (Fig. 7a) shows maximum discharge capacity of 80 mA h g^{-1} corresponding to 80% columbic efficiency over the investigated 15 cycles with a capacity fade of 0.6 mA h g^{-1} per cycle and stabilizes at around 80 mA h g^{-1}. In case of maleic acid assisted $LiCo_{0.25}Ni_{0.25}Mn_{1.5}O_4$ (Fig. 7b), the cells deliver stable discharge capacities of around 84 mA h g^{-1} with capacity fade of 0.5 mA h g^{-1} per cycle respectively. Already researcher [32] had reported on synthesis of cobalt and nickel doped spinels but cycled only up to 4.4V delivering inferior capacities. Wu et al. [33] investigated $LiMn_{1.5}Ni_{0.2}Co_{0.3}O_4$ delivering capacity of 100 mA h g^{-1} with a capacity fade of 0.2 mA h g^{-1} per cycle over the investigated 15 cycles. Rojas et al. [34] reported that $LiNi_{0.25}Co_{0.5}Mn_{1.25}O_4$ was synthesized through combustion method and delivered maximum discharge capacity of 98 mA h g^{-1} with capacity fade of 0.5 mA h g^{-1} per cycle over the investigated 15 cycles. It is interesting to observe that in the present case, oxalic acid assisted $LiCo_{0.25}Ni_{0.25}Mn_{1.5}O_4$, delivers maximum discharge capacity of 110 mA h g^{-1} than other chelating agents with good capacity retention and very low capacity fade of 0.2 mA h g^{-1} per cycle corresponding to 96% columbic efficiency. The oxalic acid undergoes complete combustion for associating with two COOH group and preventing cationic disorder.
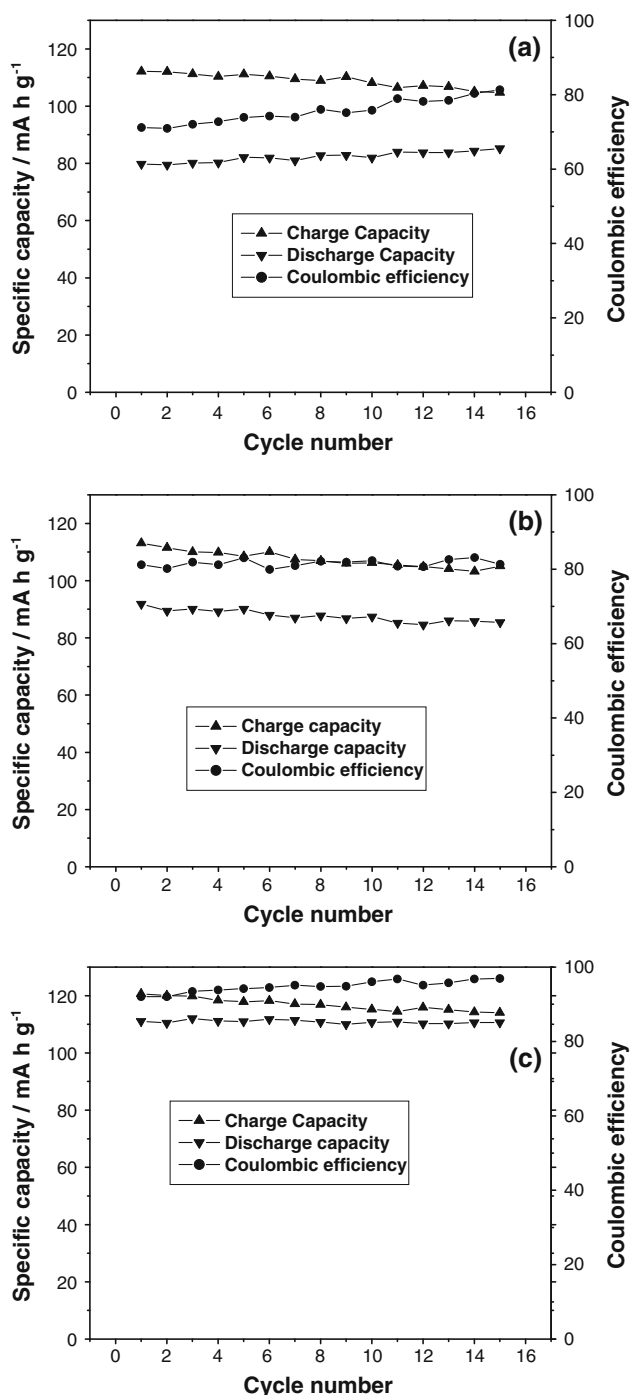
Fig. 7 The Cycling behaviour of sol–gel derived $LiCo_{0.25}Ni_{0.25}Mn_{1.5}O_4$ using **a** acetic acid, **b** maleic acid and **c** oxalic acid as chelating agents

3.6 dQ/dE versus potential curves

Figure 8 depicts the differential capacity (dQ/dE) curves of the sol–gel derived $LiCo_{0.25}Ni_{0.25}Mn_{1.5}O_4$ calcined at 850 °C using acetic acid (Fig. 8a), maleic acid (Fig. 8b) and oxalic acid (Fig. 8c) assisted chelating agents. It can be
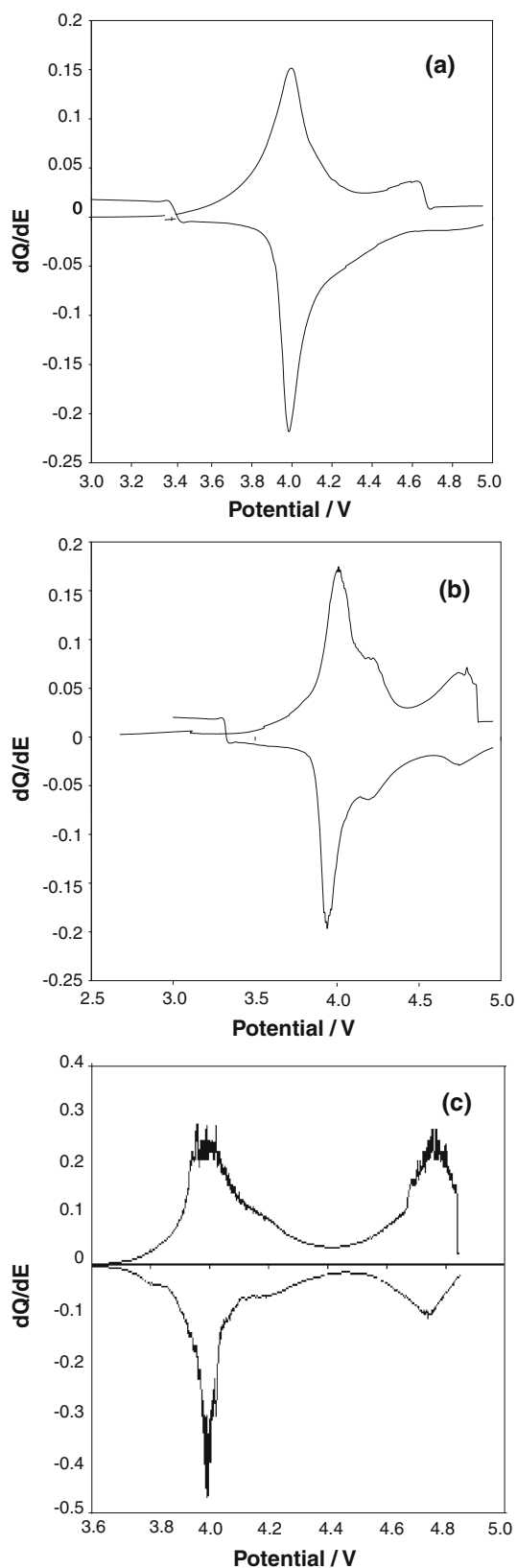
Fig. 8 The differential capacity curve of sol–gel derived of sol–gel derived $LiCo_{0.25}Ni_{0.25}Mn_{1.5}O_4$ using **a** acetic acid, **b** maleic acid and **c** oxalic acid as chelating agents

seen from (Fig. 8a) that the curve possesses three oxidative peaks occurs at around 3.8, 4 and 4.6 V during lithium ion extraction and three reductive peaks at 3.8, 4, 4.6 V for lithium insertion. These three peaks are attributed to Mn^{3+}/Mn^{4+}, Co^{3+}/Co^{4+} and Ni^{2+}/Ni^{4+} couples respectively. These results are in good agreement with previous researchers [35]. It is quite interesting to note that maleic acid (Fig. 8b) assisted $LiCo_{0.25}Ni_{0.25}Mn_{1.5}O_4$ illustrates the three anodic and cathodic peaks centered at around 4, 4.2, 4.7 V. Finally, oxalic acid (Fig. 8c) associated spinel shows two broad anodic and cathodic peaks at 4 and 4.8 V. All preliminary observations suggest that oxalic acid assisted $LiCo_{0.25}Ni_{0.25}Mn_{1.5}O_4$, bestows enhanced electrochemical stability.

4 Conclusions

$LiCo_{0.25}Ni_{0.25}Mn_{1.5}O_4$ has been synthesized via sol–gel route using three chelating agents acetic acid, maleic acid and oxalic acid to obtain single phase micron sized (0.5 μm) particles with enhanced electrochemical performance for use as an attractive 5 V cathode material in lithium rechargeable batteries. Charge–discharge studies of $LiCo_{0.25}Ni_{0.25}Mn_{1.5}O_4$ spinels synthesized using oxalic acid delivers a stable discharge capacities of 110 mA h g^{-1} when cycled from 3 to 5 V over the investigated 15 cycles with very low capacity fade of 0.2 mA h g^{-1} per cycle corresponding to 96% columbic efficiency. Therefore, we may conclude that oxalic acid assisted $LiCo_{0.25}Ni_{0.25}Mn_{1.5}O_4$ spinel could be an apt high voltage cathode material for delivering high discharge capacity with good capacity retention for use in lithium rechargeable batteries.

References

1. Kawai H, Nagata M, Tukamoto H, West AR (1999) J Power Sources 81:72
2. Broussely M, Archdale G (2004) J Power Sources 136:394
3. Fonseca CP, Neves S (2004) J Power Sources 135:254
4. Shukla AK, Prem Kumar T (2008) Curr Sci 94:314
5. Kim JH, Yoon CS, Sun YK (2004) Electrochem Solid State Lett 7:220
6. Yang MH, Fang JC, Yeh SF, Tsai JH, Wu HC (2004) 5th advanced batteries and accumulators, ABA
7. Gopukumar S, Schlorb H, Rahner D (2001) Mater Chem Phys 70:123
8. Wohlfahrt-Mehrens M, Vogler C, Garche J (2004) J Power Sources 127:64
9. Gummow RJ, de Kock A, Thackeray MM (1994) Solid State Ionics 69:67

10. Arora P, Popov BN, White RE (1998) J Electrochem Soc 145:815
11. Thackeray MM, Shao-Horn Y, Kahaian A, Kepler KD, Skinner E, John Vaughey JT, Hackney SA (1998) J Electrochem Soild State Lett 1:19
12. Tarascon JM, McKinnon WR, Coowar F, Bowmer TN, Amatucci GG, Guyomard D (1994) J Electrochem Soc 141:1431
13. Park SB, Eom WS, Cho WI, Jang H (2006) J Power Sources 159:684
14. Ohzuku T, Takeda S, Iwanaga M (1999) J Power Sources 81:94
15. Thirunakaran R, Kim KT, Kang YM, Seo CY, Lee JY (2004) J Power Sources 137:104
16. Thirunakaran R, Kim KT, Kang YM, Seo CY, Lee JY (2005) J Mater Res Bull 40:186
17. Thirunakaran R, Sivashanmugam A, Gopukumar S, Dunnill CW, Gregory DH (2008) J Phys Chem Solids 69:2090
18. Thirunakaran R, Sivashanmugam A, Gopukumar S, Dunnill CW, Gregory DH (2008) Mat Res Bull 43:2129
19. Thirunakaran R, Sivashanmugam A, Gopukumar S, Rajalakshimi R (2009) J Power Sources 187:574
20. Thirunakaran R, Sivashanmugam A, Gopukumar S, Dunnill CW, Gregory DH (2008) J Mater Process Technol 208:531
21. Rajakumar S, Thirunakaran R, Sivashanmugam A, Yamaki J, Gopukumar S (2009) J Electrochem Soc 156:A252
22. Sebastien P, Lucas S, Helene L, Yvan R, Carole B, Severine J, Frederic L, Sebastien M (2008) Electrochim Acta 53:4137
23. Gao Y, Myrtle K, Zhang M, Reimers JN, Dahn JR (1996) Phys Rev B 54:3883
24. Benedek R, Johnson CS, Thackeray MM (2006) Electrochem Solid State Lett 9:A291
25. Tsai YW, Santhanam R, Hwang BJ, Hu SK, Sheu HS (2003) J Power Sources 119:705
26. Arunkumar TA, Manthiram A (2005) Electrochem Solid State Lett 8:A405
27. Okada M, Lee YS, Yoshio M (2000) J Power Source 90:200
28. Sahan H, Goktepe H, Patat S (2008) Neorg Mater 44:493
29. Shinova E, Stoyanova R, Zhecheva E, Ortiz GF, Lavela P, Tirado JL (2008) Solid State Ionics 179:2208
30. Yan H, Huang X, Lu Z, Huang H, Xue R, Chen L (1997) J Power Sources 68:532
31. Mauger A, Gendron F, Amdoni N, Zarrouk H, Julien CM (2006) Mater Sci Eng B 129:75
32. Ammundsen B, Burns GR, Islam MS, Kanoh H, Roziere J (1999) J Phys Chem B 103:5180
33. Wu HM, Tu JP, Yuan YF, Xiang JY, Chen XT, Zhao XB, Cao GS (2007) J Electroanal Chem 608:16
34. Rojas RM, Amarilla JM, Pascual L, Rojo JM, Kovacheva D, Petrov K (2006) J Power Sources 160:535
35. Kitato H, Fujihara T, Takeda K, Nakanishi N, Nohma T (2005) Solid State Lett 8:A90